
THREE PHASE SQUIRREL CAGE INDUCTION MOTOR WITH DEEP ROTOR BARS IN TRANSIENT BEHAVIOUR: A PERFORMANCE ANALYSIS

By

Eyenubo Ogheneakpobo Jonathan and Anamonye Uzonna Gabriel

^{1,2}Department of Electrical/Electronic Engineering

Delta State University, Odeh Campus,

Nigeria

Email: eyenubo63@yahoo.com

ABSTRACT

The rotor parameters, the resistance and the leakage inductance, vary with the currents frequency of rotor bars due to skin effect, and for small frequencies can be negligible (under 10 15 Hz); but for higher frequencies this variation of the parameters cannot be negligible. In this paper, for higher frequencies some analytic expressions are proposed, that result from the skin effect theory, for the rotor resistance and for the leakage inductance. The simulations were done by SYMNAP – Symbolic Modified Nodal Analysis Program, a program that can determine, in a full-symbolic form the voltages and the currents for the equivalent scheme for one phase of the asynchronous motor. Symbolic expressions for the characteristics quantities of the general regime of the induction motor allow graphic representation for different parameters. These analytic expressions allow a more accurate analysis of asynchronous motor performance for different drive systems. To simulate the dynamic (transient) behaviour of the induction motor, Park-Blondel equations have been used; these equations have a nonlinear form due to both their structure and frequency variation of the rotor parameters. The integration of these equations is performed with the help of the integration routines for ordinary differential equations in Matlab programming environment. It was found that the nominal values of the quantities that characterize the induction motor operation, obtained by simulation, practically coincide with the values from the catalogue.

Keywords: *Induction Motor, State Equations, Transient Behaviour, Deep Rotor Bars*

INTRODUCTION

Numerous studies have been made on estimating the electrical parameters of the asynchronous machine given both skin effect, and the saturation level. For the electrical drives with three phase induction motors with deep rotor bars were developed mathematical models and command strategies for developing high performance systems [1-2]. In electrical drives, it is preferred the vector command in respect to the rotor flux, a flux that cannot be defined using one form for motor with deep rotor bars; as a result, in many cases

it is used the air gap flux for the vector command. Using the pseudo rotor-flux, it can be achieved similar performances as with the rotor flux orientation, in this case, the equivalent rotor parameters are used. The squirrel cage with deep rotor bars can be equivalent with a double cage, one of these cages having constant parameters [3].

Based on the influence of the skin effect over electrical rotor parameters can be constructed a mathematical model for the asynchronous motor with deep rotor bars that allows simulation of different

operating modes are presented in this paper. It is considered constant stator current frequency, equal to the network frequency at which the motor is fed. Rotor parameters are considered constant, independent of the rotor current frequency, for values between 0 and 10...15 Hz. For higher frequencies, analytic expressions are proposed, that result from the skin effect theory, for the rotor resistance and leakage inductance, a program that allows complete symbolic determination of the branch voltages and currents of the equivalent scheme corresponding to one phase of the induction motor. In order to simulate the induction motor in the transient (dynamic) behaviour we use the Park-Blondel equations

$$u_{sk} = R_s i_{sk} + j\check{S}_k \mathcal{E}_{sk} + \frac{d\mathcal{E}_{sk}}{dt} \tag{1a}$$

$$\Rightarrow \left\{ \begin{aligned} u_{sd} &= R_s i_{sd} - \check{S}_1 \mathcal{E}_{sq} + \frac{d\mathcal{E}_{sd}}{dt} \\ u &= R_s i_{sq} + \check{S}_1 \mathcal{E}_{sd} + \frac{d\mathcal{E}_{sq}}{dt} \end{aligned} \right\} \tag{1b}$$

$$\mathcal{E}_{sk} = L_{s+} i_{sk} + L_- i_{-k} \Rightarrow \left\{ \begin{aligned} \mathcal{E}_{sd} &= L_{s+} i_{sd} + L_- i_{-d} \\ \mathcal{E}_{sq} &= L_{s+} i_{sq} + L_- i_{-q} \end{aligned} \right\} \tag{1c}$$

$$0 = R_r i_{rk} + j(\check{S}_k - \check{S}) * \mathcal{E}'_{rk} + \frac{d\mathcal{E}'_{rk}}{dt} \tag{1d}$$

$$\left\{ \begin{aligned} 0 &= R_r i_{rd} - (\check{S}_1 - \check{S}) * \mathcal{E}'_{rk} + \frac{d\mathcal{E}'_{rd}}{dt} \\ 0 &= R_r i_{rq} + (\check{S}_1 - \check{S}) * \mathcal{E}'_{rd} + \frac{d\mathcal{E}'_{rq}}{dt} \end{aligned} \right\} \tag{1e}$$

$$\mathcal{E}'_{rk} = L'_{r+} i_{rk} + L_- i_{-k} \Rightarrow \left\{ \begin{aligned} \mathcal{E}'_{rd} &= L'_{r+} i_{rd} + L_- i_{-d} \\ \mathcal{E}'_{rq} &= L'_{r+} i_{rq} + L_- i_{-d} \end{aligned} \right\} \tag{1f}$$

$$J \frac{d\Omega}{dt} = J \frac{d\check{S}}{Pdt} = \dots \tag{1g}$$

$$M = \frac{3}{2} P |\mathcal{E}_{sd} i_{sq} - \mathcal{E}_{sq} i_{sd}|; \check{S}_k = \check{S}_1 \tag{1h}$$

The general coordinate system K , which has the angular velocity \check{S}_k in respect to the stator coordinate system, is particularized for the synchronous

[4]. These equations have a nonlinear form due to both their structure and the variation of the rotor parameters in respect of the frequency. The integration of these equations is performed with the help of the integration routines for ordinary differential equations in Matlab programming environment.

The Mathematical Model of the Induction Motor

The mathematical model of the induction motor used for any behaviour is elaborated in synchronous coordinate (Park-Blondel equations) and is presented as it follows:

coordinate with speed \check{S}_1 , this means that $\check{S}_k = \check{S}_1$.

In the system equations (1) the rotor cage parameters R_r' and $L_{r\uparrow}'$ dependent on the rotor bars angular frequency \check{S}_r , and the others electrical parameters are constants. If the simulations are performed for only one stator frequency (such as nominal stator frequency) the parameters R_r' and $L_{r\uparrow}'$ vary with the slip s . For simulations at different stator frequencies is absolutely necessary that the rotor parameters are function of the angular frequency of the currents from the rotor bars

\check{S}_r , for the stator frequency of $f_1 = 50\text{Hz}$, and $s = 1$, the influence of the skin effect is negligible, that means the dependence on the slip s is not relevant [5- 6].

Rotor Electrical Parameters

The skin effect analysis shows that the rotor resistance R_r' reported at the stator increases with, and $\sqrt{\check{S}_r}$ leakage inductance $L_{r\uparrow}'$ decreases with $\sqrt{\check{S}_r}$. Therefore, the rotor parameters reported at the stator can be written as it follows:

$$\left(\begin{array}{l} R_r'(\check{S}_r) = R_r' = ct. \quad \text{for } \check{S}_r \in (0; \check{S}_{rr}) \\ R_r'(\check{S}_r) = k_1 + k_2\sqrt{\check{S}_r}; \text{ for } \check{S}_r > \check{S}_{rr} \\ L_{r\uparrow}'(\check{S}_r) = L_{r\uparrow}' = ct. \quad \text{for } \check{S}_r \in (0; \check{S}_r) \\ L_{r\uparrow}'(\check{S}_r) = K_3 - \frac{K_4}{\sqrt{\check{S}_r}}; \check{S}_r > \check{S}_{rr} \end{array} \right) \quad (2)$$

The constants K_1 , K_2 , K_3 and K_4 are determined from the continuity condition at the point $\check{S}_r = \check{S}_{rx}$ and calculation of the electrical parameters for the squirrel cage at starting point ($s = 1$), these parameters are obtained from the catalogue data. Till the pulsation is $\check{S}_r = \check{S}_{rx}$, the rotor parameters are considered constant, and for $\check{S}_r > \check{S}_{rx}$ the rotor parameters vary with pulsation \check{S}_r according to relations (2). These are valid for a wide range of frequency from rotor circuit [7].

Rotor Parameters at Starting

Rotor squirrel cage is made with deep bars, parameters R_r' and $L_{r\uparrow}'$ vary in large limits when the rotor angular frequency \check{S}_r takes values between 0 and \check{S}_1 ; at the starting ($n = 1$), the rotor angular frequency \check{S}_r is equal to the stator angular frequency ω_1 , in this case the skin effect is strong ($\check{S}_1 = 2f \cdot 60$). The catalogue data for the analyzed induction motor are presented in table 1 with the known notations.

Table 1: The Catalogue data for the Motor

P_n [kW]	U_n [V]	I_n [A]	n_1 [rot/min]	N [rot/min]	η_n [%]
$\cos \phi_{ln}$	i_p -	m_p -	m_m -	J [kgm ²]	Star connection

Based on these data the following quantities can be calculated: P_n, s_n, M_n, S_n . Next step for the calculation of the starting parameters is: the starting impedance Z_p , the rotor resistance at starting point R'_{rp} and the leakage inductance at starting point $L'_{r\uparrow}$

.In the computation process the rated impedance Z_n is used. Using the known relations from the asynchronous motor theory, for $n = 0$, the rotor resistance R'_{rp} is computed, thus [8-9]:

$$s = 1 \Rightarrow Z_p = \frac{U_{fn}}{I_p} = \frac{U_{fn}}{i_p I_{fn}} = \frac{Z_h}{i_p} \tag{3a}$$

$$Z_h = \frac{U_{fn}}{I_{fn}}; M = \frac{P_{J1}}{\Omega_{1s}} = \frac{3R'_r I_2^2}{\Omega_{1s}}$$

$$s = 1 \Rightarrow M_p = \frac{3R'_{rp} I_{rp}^2}{\Omega_1} \cong \frac{3R'_{rp} I_{sp}^2}{\Omega_1}; (I_{so} \cong 0 \Rightarrow I'_{rp} = I_{rp})$$

$$\frac{M_p}{M_n} = m_p \cong \frac{3R'_{rp} I_{sp}^2 \Omega_n}{\Omega_1 M_n \Omega_n} = \frac{3R'_{rp} I_{sp}^2}{P_n} (1 - s_n) \Rightarrow \tag{3b}$$

$$R'_{rp} = \frac{m_p P_n}{3(1 - s_n) * (i_p I_{fn})^2}$$

The values of the parameters $Z_p, R_s, L_{s\uparrow}, R'_{rp}$ are known and the leakage inductance $L'_{r\uparrow}$ can be calculated, at starting point, with the following relation:

$$R'_r(\check{S}_r) = \left\{ \begin{array}{l} R'_r; \check{S}_r \in [0; \check{S}_{rx}] \\ \frac{R'_r \sqrt{\check{S}_1} - R'_{rp} \sqrt{\check{S}_{rx}}}{\sqrt{\check{S}_{rx}} - \sqrt{\check{S}_1}} + \frac{R'_{rp} - R'_r}{\sqrt{\check{S}_1} - \sqrt{\check{S}_{rx}}} \sqrt{\check{S}_r}; \\ \check{S}_r > \check{S}_{rx} \end{array} \right\} \tag{5a}$$

$$L'_{r\uparrow}(\check{S}_r) = \left\{ \begin{array}{l} L'_{r\uparrow}; \check{S}_r \in [0; \check{S}_{rx}] \\ \frac{\sqrt{\check{S}_1} L'_{r\uparrow} - \sqrt{\check{S}_{rx}} L'_{rp\uparrow}}{\sqrt{\check{S}_{rx}} - \sqrt{\check{S}_1}} - \frac{(L'_{r\uparrow} - L'_{rp\uparrow}) \sqrt{\check{S}_1} \sqrt{\check{S}_{rx}}}{\sqrt{\check{S}_{rx}} - \sqrt{\check{S}_1}} \frac{1}{\sqrt{\check{S}_r}} \\ \check{S}_r > \check{S}_{rx} \\ \check{S}_1 > \check{S}_{rx} \end{array} \right\} \tag{5b}$$

The last two relations in system (5) highlight the variation of the rotor parameters $R'_r(\check{S}_r)$ and $L'_{r\uparrow}(\check{S}_r)$ in respect of the \check{S}_r , due to skin effect. The

mathematical structure of the model (1), remains the same, except that the parameters R'_r and $L'_{r\uparrow}$ become $R'_r(\check{S}_r)$, and $L'_{r\uparrow}(\check{S}_r)$, respectively, according to

relation (5). For the relative rotor resistance reported to the stator R_r' is known relationship that rotor resistance

in relative unit r_r' is equal to the rated slip s_n as shown in the following relations [10]:

$$\begin{aligned}
 R_r' &= \frac{s_n(P)_n}{3I_r'^2} = \frac{s_n(P_M)_n}{3I_r'^2(1-s_n)} = \frac{s_n(P_n + P_{vf})}{3I_r'^2(1-s_n)} \cong \\
 &\frac{s_n P_n}{3I_r'^2(1-s_n)} \cong s \frac{y_n 3U_{sn} I_{sn} \cos \{s_n\}}{3(I_{sn} \cos \{s_n\})^2 (1-s_n)} \Rightarrow \\
 \Rightarrow \frac{R_r'}{Z_b} &= R_r' \frac{I_{sn}}{U_{sn}} = r_r' = s \frac{y_n}{(1-s_n) \cos \{s_n\}}; \\
 \frac{y_n}{(1-s_n) \cos \{s_n\}} &\cong 1 \Rightarrow r_r' = s_n
 \end{aligned}
 \tag{6}$$

The Study of Asynchronous Three Phase Motor with Known Parameters

In order to simulate different operating behaviour of the three phase asynchronous motor expressions obtained in

section 2.1 we will use the rated values presented in table 2 [11]:

$$\begin{aligned}
 U_{fn} &= 323.32V; I_{fn} = 130A; Z_b = Z_n = U_{fn} / I_{fn} = 2.48\Omega; f_n = 60Hz \\
 p &= 3; R_s = 0.053\Omega; R_r' = 0.0657\Omega; L_{st} = 1.034mH \\
 L_{st}' &= 0.955mH; L_- = 28.1mH
 \end{aligned}$$

Table 2: Rated Values for the Motor

P_n [kW]	U_n [V]	I_n [A]	n_1 [rpm]	N [rpm]	η_n [%]
100	560	130	1200	1168.8	0.897
$\cos \phi_{ln}$ -	i_p -	m_p -	m_m -	J [kgm ²]	Connect
0.87	4	1.1	1.813.38		Star

With the values from table 2 the next quantities are calculated: $M_n = 817$ Nm; $M_p = 898,7$ Nm; $I_p = 520$ A; $S_n = 128094,8$ VA; $s_n = 0,026$; $P_{ln} = S_n \cos \phi_{ln} = 111442,5$ W; $r_r' = 0,0262 \cong s_n = 0,026$.

It can be noticed that the last relation (6) is verified with a very good approximation. Based on relations (5) and the data in table 2 are obtained the numerical values for the electrical parameters reported to the rotor cage for $\check{S}_{rx} = 81$ rad/s; electrical parameters of the motor are:

Resisting Torque at the Motor Shaft

Load torque is required by the drive equipment (working machine) for a technological operation (turning a piece, forming by pressing, lifting an object) or other operations such as electric traction. Mechanical friction torques exists, both in electrical machine, and in working machine. It is customary that all torques that work in the opposite direction in the electrical machine-working machine system, distinct from the electromagnetic torque developed by motor, to be summed into one resultant load torque, which is called a resisting torque, a

torque that is opposing the movement. The electrical motor develops a torque M_2 at shaft which gives a stronger movement than M_r ; in steady-state $M_r = M_2$. Mechanical characteristic of the driven system represents the dependence between the load torque (resistance) M_r at the drive system shaft and a quantity

$$M_s = M_f + M_r; \tag{10a}$$

$$M_s = M_0 + (M_{sn} - M_0) * \left(\frac{\Omega}{\Omega_n} \right)^a \tag{10b}$$

where: Ω_n - the rated angular velocity; M_0 - the initial resisting torque; M_{sn} - the rated load torque; a - an exponent which can take different values, for example: $a = 0 \rightarrow M_s = M_{sn}$ constant (lifting mechanism); $a = 1 \rightarrow M_s$ linear variation with the angular velocity Ω (braking with a dc machine with

which characterizes the driven installation (the angular velocity Ω , the position angle α , the covered space etc.). In many cases the mechanical characteristic is presented as: $\Omega = f(M_s)$. An analytic expression for the mechanical characteristic can be the following expression [12-14]:

constant excitation); $a = 2 \rightarrow$ mechanical parabolic characteristic, often encountered in practice.

In railway traction, the load torque is based on the variation of traction force F_0 at the wheel rim in respect of the locomotive speed (figure 3), to which is added the dependent drag resistance R_L (figure 4) function of velocity variation.

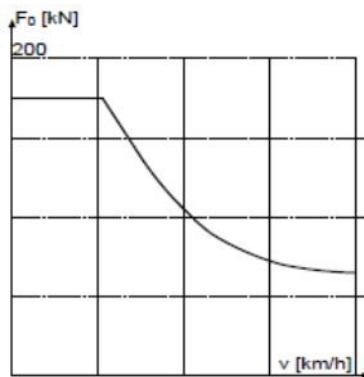


Figure 3: Variation of the drive force F_0 at the wheel rim according to the movement speed of the locomotive

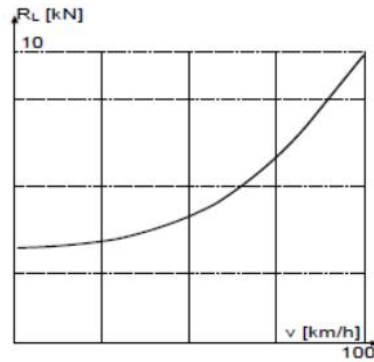


Figure 4: Variation of the R_L drags resistance depending on the speed of the locomotive

It is noted that $R_L \ll F_D$ and on this basis M_r torque at motor shaft can be approximated as shown in Figure 5.

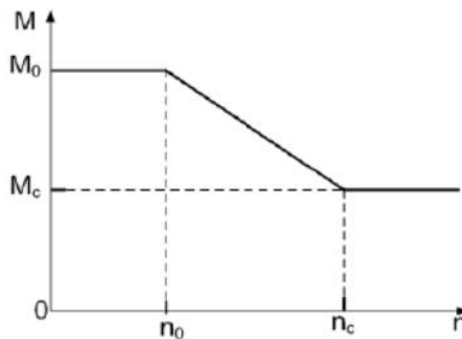


Figure 5: Variation of the resistive torque M_r at the motor shaft, function of the rotor speed n

Simulation of the Starting Process with General Mathematical Model for Rated Data and Constant Rotor Parameters

These simulations are performed for stator currents i_A, i_B, i_C , for rotor speed and electromagnetic torque. These simulations are performed at rated data for a resisting torque equal to the electromagnetic torque

and variable rotor parameters. The induction motor can start at rated torque due to the skin effect which increases rotor resistance and the starting torque. The results of the simulations are presented in figures 6, 7, 8. The application of digital filter velocity and comparison at different torques and periods are in 9 and 10.

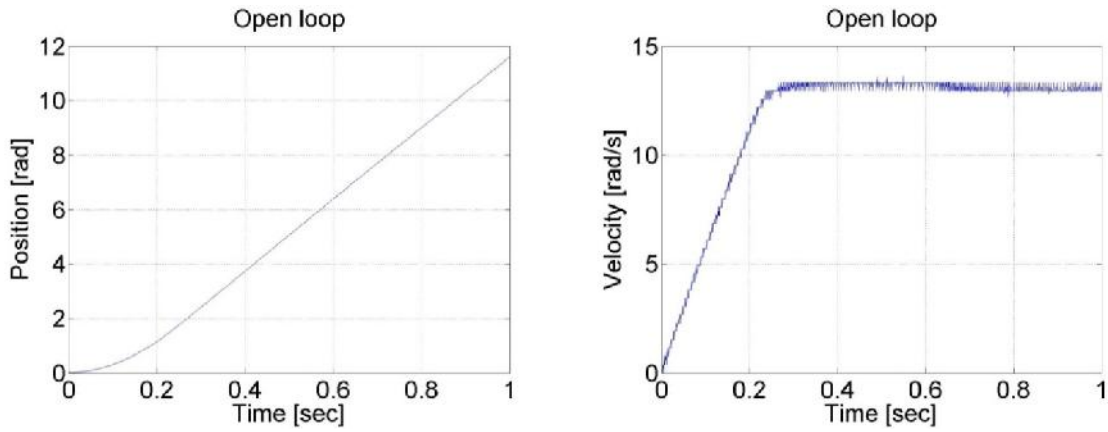


Figure 6: Open loop control Torque = 1

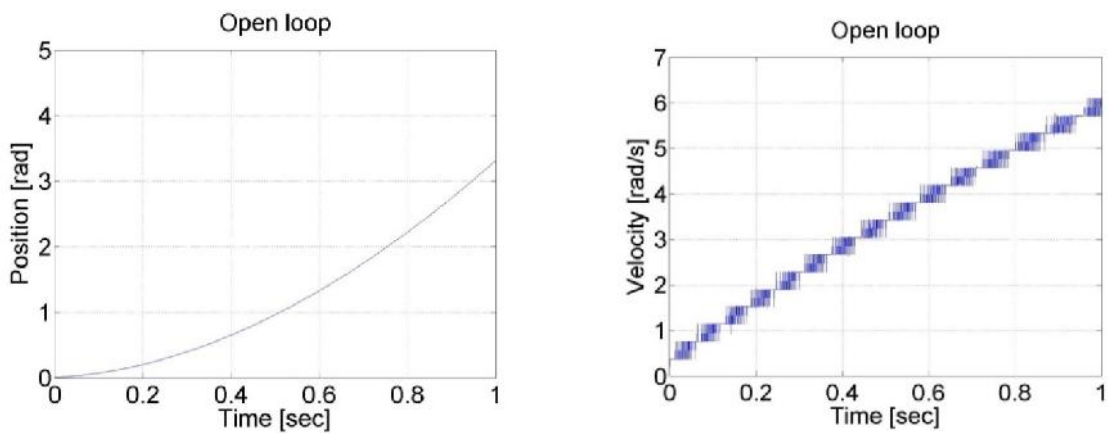


Figure 7: Open loop control Torque = 0.1

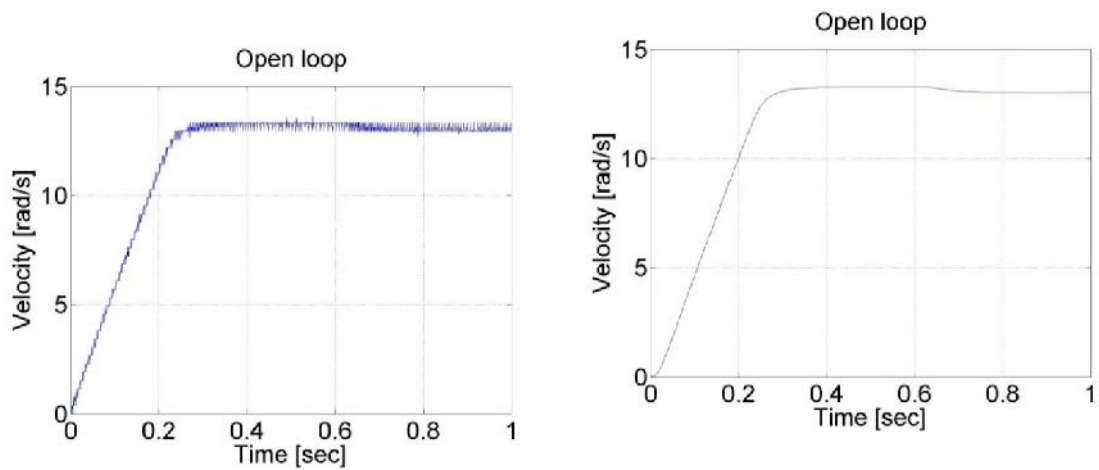


Figure 8: Comparison of unfiltered and filtered velocity

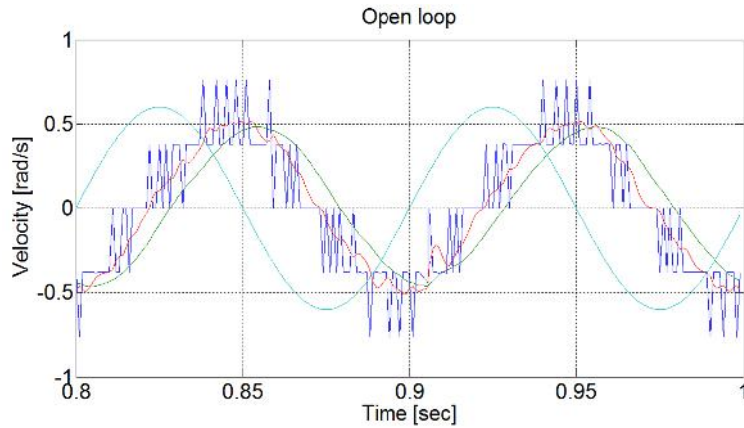


Figure 9: Comparison of digital filters period 0.1 s;
light blue, unfiltered: blue, normal filter: green

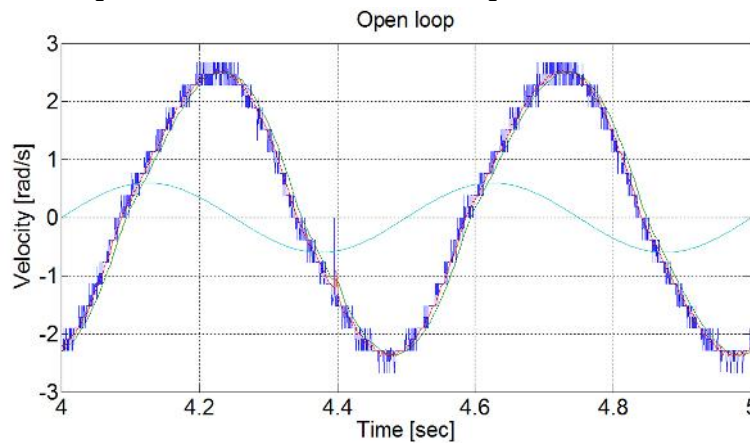


Figure 10: Comparison of digital filters period 0.4 s.
light blue, unfiltered: blue, normal filter: green

References:

- [1] Repo A.-K., Rasilo P., and Arkkio A. (2008), 'Dynamic electromagnetic torque model and parameter estimation for a deep-bar induction machine', IET Elect. Power Appl., vol. 2, No. 3, pp. 183 -192
- [2] Levi E., (1996), Main flux saturation modeling in double-cage and deep-bar induction machines, IEEE Trans. Energy Conversion, vol. 11, No. 2, pp.305 - 311
- [3] Pedra J, Sainz L, (2006), 'Parameter estimation of squirrel-cage induction motors without torque measurements', IEE Proc. Elect. Power Appl., vol. 153, no.2, pp. 87 -94
- [4] Verghese G. C., Lang J. H., and Å Onder M. K., (1999), 'Generalizing the Blondel-Park transformation of electrical machines: Necessary and sufficient conditions', IEEE Trans. Circuits and Systems, Vol. 36, No. 8, 1058-1067
- [5] Atkinson D.J., Finch J.W. and Acarnley P.P., (1996), 'Estimation of rotor resistance in induction motors, IEE Proc. Elect', Power Appl., vol. 143, no.1, pp. 87 -94
- [6] Rik W.A and De Doncker A., (1992), 'Field-Oriented Controllers with Rotor Deep Bar Compensation Circuits', IEEE Trans. Industry Applications, vol. 28, No. 5, pp. 1062 - 1070
- [7] Jul-Ki Seok, and Seung-Ki Sul, (1998), 'Pseudo rotor-Flux-Oriented Control of an Induction Machine for Deep-Bar-Effect Compensation', IEEE Trans.

- Industry Applications, vol. 34, No. 3, pp. 429 – 434
- [8] Anderson P.M. and Fouad A.A., (2003), 'Rotating (D-Q) Transformation and Space Vector Modulation Basic Principles', McGraw- Hill Companies INC
- [9] Park R.H., (1989), '*Two Reaction Theory of Induction Machines*', AIEE Transactions 48:716-730
- [10] Vaimann T, Kallaste A, and Kilk A, (2011), 'Sensor less Detection of Induction Motor Rotor Faults Using the Clarke Vector Approach', *Scientific Journal of Riga Technical University: Power and Electrical Engineering* 29 4-21.
- [11] Ansari A A, and Deshpande D M, (2010), 'Mathematical Model of Asynchronous Machine in MATLAB Simulink', A. Ansari et. al. / International Journal of Engineering Science and Technology Vol. 2(5), 1260-1267
- [12] Blödt M, Granjon P, and Raison B, (2008), 'Models for Bearing Damage Detection in Induction Motors Using Stator Current Monitoring', IEEE TRANSACTIONS ON INDUSTRIAL ELECTRONICS, VOL. 55, NO. 4, APRIL 2008
- [13] Arya M K, and Wadhvani S, (2009), 'Transient Analysis of Three Phase Squirrel Cage Induction Machine using Matlab', International Journal of Engineering Research and Applications (IJERA) ISSN: 2248-9622, Vol. 1, Issue 3, pp.918-922.
- [14] Yu L and Wong KN (1989), '*Open and Short Circuit Behavior of Induction Motors*', (IEEE Conference Publications) 35-40.